Modeling of a Polymer 1 × 3 MMI Power Splitter for Optical Backplane

Atef M. Rashed and David R. Selviah
Department of Electronic and Electrical Engineering
University College London, Torrington Place,
London WC1E 7JE, United Kingdom
Telephone: +44 20 7679 3056, Fax: +44 20 7388 9325
Email: a.rashed@ee.ucl.ac.uk
Email: d.selviah@ee.ucl.ac.uk

***Abstract*—A 0.4 dB excess loss, 0.01 dB output channel imbalance polymer 1 × 3 MMI power splitter is modeled having linearly tapered input section suitable for use in an optical backplane connector. The device design was additionally optimized using FD-BPM to have a good tolerance to source lateral misalignments.**

Keywords - polymer MMI; power splitter; optical backplane; multimode tapered waveguide; spot size converter; FD-BPM; source misalignmen; optical connector

I. INTRODUCTION

Large electronic systems are generally constructed as racks of many dismountable printed circuit boards (PCBs) plugged into a larger PCB at the back of the rack, known as the backplane or motherboard. The backplane has data buses to interconnect the PCBs at high data rates using copper tracks. At current data rates of 10 Gb/s [1] copper tracks can only be used over short distances and this requires complex signal shaping to overcome attenuation and distortion due to high frequency parasitics and limited bandwidth [1]. High bandwidth optical polymer waveguides integrated within the FR4 PCB layer offer a low cost and compact approach to overcome the limitations of copper track interconnects [2, 3]. Due to the complex layout of interconnects on the PCBs and on the backplane, there is a growing need for polymer waveguide devices integrated onto the optical backplane for optical signal processing and distribution. Multimode interference (MMI) optical power splitters [4] are an important example of such devices for signal distribution to aid routing on the optical backplane.

Vertical cavity surface emitting lasers (VCSELs) used as signal sources on the dismountable PCBs must be aligned to the optical backplane at optical connectors. However, low cost connectors may suffer from some misalignment of the VCSEL relative to the waveguide.. Therefore, the waveguide should be designed to provide uniform and preferably high source coupling efficiency even when the optical source is offset [5]. This can be achieved for lateral offsets using laterally tapered input waveguides [6] as part of the optical connector. In this paper FD-BPM [7] is used to design a polymer 1 × 3 MMI power splitter with tapered input waveguide for use in the optical connector.

II. PRINCIPLE OF MMI SPLITTER

MMI devices are useful photonic components because they can reproduce images of an input beam at periodic intervals along the propagation direction due to interference of the waveguide modes. This self-imaging principle [8] causes the input field to be reproduced as either single or multiple images at regular intervals along the length of the MMI device. In a straight-sided MMI device, single and double images of the input field occur at integer and odd half-integer multiples of $3L_\pi$, respectively [8]. 3-fold images of the input field also occur at $L_\pi/4$, where L_π is the beat length of the two lowest-order modes in the MMI device and is defined to be [8]:

$$L_\pi = 4nW^2/3\lambda \quad (1)$$

where n is the waveguide core refractive index, W is the width of the MMI region and λ is the free space wavelength.

The length of the MMI device can be reduced without compromising the performance by considering structures with a smaller or a parabolically tapered width that still offer a uniform output power distribution [9].

III. 1 × 3 MMI POWER SPLITTER

Our final waveguide design after optimization using FD-BPM has a 21 μm wide input waveguide that tapers down linearly with a half taper angle of 1.6º over a length of 250 μm. It joins our 292 μm long, non-uniform width MMI section at the centre of its input port. Our MMI section width is 23 μm at both input and output edges and narrows to a 19 μm waist at the middle of the structure. The side walls of the MMI section are circular arcs with radii of curvature of 6 mm that make an angle of up to 1.4º with the optical propagation axis as shown in Fig. 1(a). The MMI section is followed by three output waveguides arranged in a fan, each of 7 μm width. One output waveguide is 258 μm long and is aligned to the longitudinal axis of the device. The outer two waveguide centers are positioned symmetrically at ±15 μm either side of the central

axis with ±0.7º tilt angle to the longitudinal axis and their ends are aligned with the end of the central waveguide. The waveguides have core and cladding refractive indices of 1.54 and 1.52, respectively. The material loss of the waveguide is taken to be 0.03 dB/cm at 850 nm wavelength. These figures are typical values for waveguide polymers used in optical backplanes such as Truemode™ polymer [10].

VCSELs for optical backplanes operating at 10 Gb/s often have 7 μm diameter apertures [1]. In our modeling we chose such a VCSEL emitting in its fundamental transverse mode as the input source. The input field used in the simulation, shown in the inset of Fig. 2, is TE-polarized with a width of 7 μm at e^{-1} intensity. The input field is launched initially at the centre of the input aperture of the input waveguide along the optical propagation z-axis direction. Fig. 1(a) shows the layout of the waveguide structure with simulation results for discrete intensity profiles of the propagating optical field at intervals along the propagation direction. Fig. 1(b) shows the corresponding intensity contour map of the propagating field.

Following our FD-BPM optimization procedure our MMI section is 8% shorter than that in the corresponding straight-sided device. This was achieved by adjusting the device dimensions to give the minimum imbalance corresponding to the greatest uniformity between the outputs of the three output waveguides whilst maintaining only a small angle between the side walls of the MMI section and the propagation axis of the device [9] to minimize excess loss.

IV. Numerical Model

The numerical model used 2-dimensional semi-vectorial FD-BPM (2D SV FD-BPM). The 2D SV wave equation for the TE-polarized optical field, u, [11] omits the dependence on the transverse direction, y, due to the structures uniformity in this direction:

$$\frac{\partial u}{\partial z} = \frac{i}{2\bar{k}}\left\{\frac{\partial}{\partial x}\left[\frac{1}{n^2}\frac{\partial}{\partial x}\left(n^2 u\right)\right] + \left(k^2 - \bar{k}^2\right)u\right\} \qquad (2)$$

where x and z are the coordinates corresponding to the lateral and propagation directions, respectively. $\bar{k}$ is the reference wavenumber and $k = (2\pi/\lambda)\, n(x, z)$ is the spatially dependent wavenumber. Since the waveguide structure supports multimode propagation the wide-angle form of SV FD-BPM incorporating the Padé approximation is employed to overcome the paraxial nature of the wave equation [12, 13]. The Padé (1, 1) approximant has been used and transparent boundary conditions (TBC) [14] were implemented in the calculations to eliminate spurious reflections at the edges of the computation domain [15]. This modeling technique only considers forward propagating waves and does not take into account reflected waves.

A 2D mesh with step sizes of Δx = 50 nm and Δz = 1 μm was used for calculations and (2) was integrated forwards in z by replacing the partial derivatives with their finite difference approximations [16]. The step sizes were chosen to be sufficiently small that they gave consistent solutions as those obtained for smaller step sizes, and that they were sufficiently large to minimize computational time. The optical field was successively calculated at each longitudinal step, Δz until reaching the end of the waveguide structure. The total power within the waveguide was determined by computing the integral of the power in the field at the corresponding z-position over the waveguide cross sectional area.

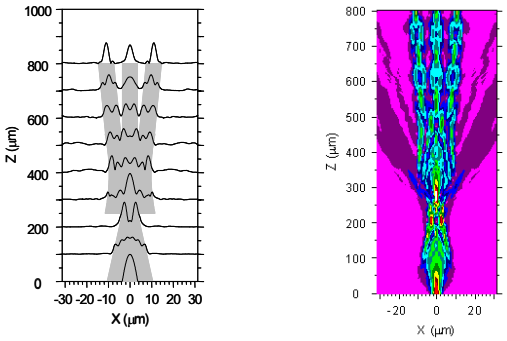

(a) (b)

Figure 1. (a) 1 × 3 MMI splitter with intensity profiles of the optical field

(b) Contour map of the propagating field intensity

V. Discussion and Results

Fig. 2 shows the near field at the end of the tilted fanned waveguides showing the uniformity of the power in the three branches. 7 μm wide extension long straight waveguides parallel to the device longitudinal z-axis were added in the simulation to each output branch to monitor the uniformity of the splitter as a function of propagation distance as signals will travel longer distances on a backplane. Fig. 3 shows the output power normalized to the input power as a function of the propagation distance. The device achieves a uniform splitting ratio of 30% in each branch. This is close enough to the ideal value of 33.3% and does not change over the propagation distance from the splitter output. However, the splitting ratio can be improved at the expense of uniformity by changing the design slightly.

The excess loss of the splitter is defined as [17]:

$$EL = -10\, log_{10}(P_{out}/P_{in}) \qquad (3)$$

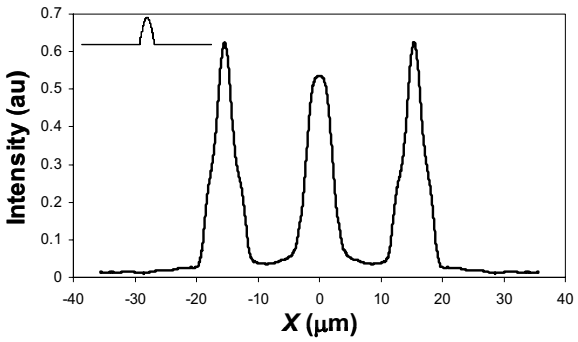

Figure 2. Output near field with inset of input field

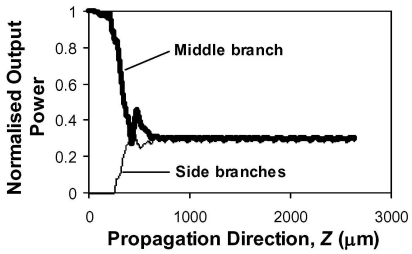

Figure 3. Normalized output power versus propagation distance

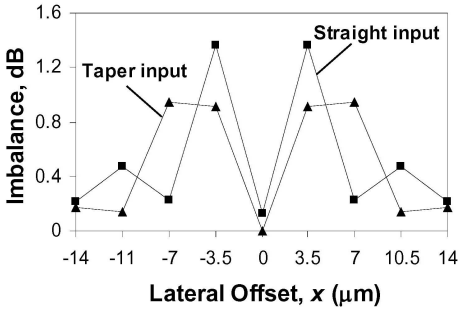

Figure 4. Imbalance versus source lateral offset

where P_{out} is the total output power of the three ports and P_{in} is the input power. The calculated *EL* is found to be as low as 0.4 dB at the end of the fanned output waveguides. A slightly higher *EL* value of 0.6 dB was calculated at the end of the extension waveguides due to the modal mismatch between the parallel extension waveguides and the fanned waveguides. However, in practice smooth bends would be used to join these to reduce such loss. These computed *EL* values also include the material loss that accumulates with distance.

The imbalance of the splitter can be defined as [18]:

$$IB = -10\ log_{10}(1-\sigma_p) \quad (4)$$

where σ_p is the standard deviation of the power at the output ports normalized to one third of the input power.

A very small *IB* of 0.01 dB at the splitter output was calculated. Hence our design achieves lower excess loss and better uniformity than the corresponding parabolic-sided one [17].

However, our circular arc-sided MMI section is 15% longer than the equivalent parabolic-sided design since the average width of the circular arc-sided design is larger than that of the parabolic-sided design and there is a direct proportionality between the average width, *W* and the beat length, L_π, of the MMI section, (1). This slight increase in the length of our design has been traded-off for less loss since losses increases as the curvature of the sides becomes sharper as in the case of the parabolic-sided design.

The effect of source lateral misalignment on the splitter output imbalance for a tapered input waveguide and a straight input waveguide of 7 μm width was compared. Fig. 4 shows that the splitter with the tapered input waveguide has less imbalance by up to 0.4 dB than the splitter with the straight input waveguide over a source lateral misalignment range of 28 μm.

VI. CONCLUSIONS

A 0.4 dB excess loss, 0.01 dB output channel imbalance polymer 1 × 3 MMI power splitter is modeled using FD-BPM. The splitter has a linearly tapered input section that provides a good tolerance to source lateral misalignments when used in optical backplane.

ACKNOWLEDGMENT

UK EPSRC, DTI and Xyratex, Havant are acknowledged for support through the LINK Storlite project.

REFERENCES

[1] F. Mederer, R. Michalzik, J. Guttmann, H.-P. Huber, B. Lunitz, J. Moisel, and D. Wiedenmann, "10 Gb/s data transmission with TO-packaged multimode GaAs VCSELs over 1 m long polymer waveguides for optical backplane applications," *Opt. Comms.*, vol. 206, pp. 309–312, June 2002.

[2] D. Israel, R. Baets, M. J. Goodwin, N. Shaw, M. D. Salik, and C. J. Groves-Kirkby, "Comparison of different polymeric multimode star couplers for backplane optical interconnect," *J. Lightwave Technol.*, vol. 13, No. 6, pp. 1057-1064, June 1995.

[3] J. Moisel, "Optical backplane for avionic applications using polymer multimode waveguides," *Proc. Of IEEE LEOS Conf.*, Paper WT1, vol. 2, pp. 567-568, 2000.

[4] M. L. Mašanović, E. J. Skogen, J. S. Barton, J. M. Sullivan, D. J. Blumenthal, and L. A. Coldren, "Multimode interference-based two-stage 1 × 2 light splitter for compact photonic integrated circuits," *IEEE Photon. Technol. Lett.*, vol. 15, No. 5, pp. 706-708, May 2003.

[5] W. B. Joyce, and B. C. DeLoach, "Alignment of Gaussian beams," *Appl. Opt.*, vol.23, No. 23, pp. 4187-4196, Dec. 1984.

[6] A. M. Rashed, and D. R. Selviah, "Modelling of polymer taper waveguides for optical backplane," *Proc. Of Semiconductor and Integrated Optoelectronics Conf.*, Cardiff, Paper 40, April 2004.

[7] A. M. Rashed, K. A. Williams, P. J. Heard, R. V. Penty, and I. H. White, "Tapered waveguide with parabolic lens: theory and experiment," *Opt. Eng.*, vol. 42, No. 3, pp. 792-797, March 2003.

[8] L. B. Soldano, and E. C. M. Pennings, "Optical multi-mode interference devices based on self-imaging: principles and applications," *J. Lightwave Technol.*, vol. 13, No. 4, pp. 615-627, April 1995.

[9] D. S. Levy, R. Scarmozzino, and R. M. Osgood, Jr., "Length reduction of tapered N × N MMI devices," *IEEE Photon. Technol. Lett.*, vol. 10, No. 6, pp. 830-832, June 1998.

[10] C. Berger, R. Beyeler, G.-L. Bona, R. Dangel, L. Dellmann, P. Dill, F. Horst, M. A. Kossel, C. Menolfi, T. Morf, B. Offrein, M. L. Schmatz, T. Toifl, and J. Weiss, "Optical links for printed circuit boards," *Proc. Of IEEE LEOS Conf.*, vol. 1, pp. 61-62, 2003.

[11] A. M. Rashed, and D. R. Selviah, "Modelling of the effects of thermal gradients on optical propagation in polymer multimode tapered waveguides in optical backplanes," *SPIE Proc. of Software and Modelling in Optics*, Photonics North 2004, Paper 5579B-54, Canada, Sept. 2004.

[12] I. Ilić, R. Scarmozzino, and R. M. Osgood, Jr., "Investigation of the Padé approximant-based wide-angle beam propagation method for

accurate modeling of waveguideng circuits," *J. Lightwave Technol*., vol. 14, No. 12, pp. 2813-2822, Dec. 1996.

[13] Y.-P. Chiou, and H.-C. Chang, "Analysis of optical waveguide discontinuities using the Padé approximants," *IEEE Photon. Technol. Lett.*, vol. 9, No. 7, pp. 964-966, July 1997.

[14] G. R. Hadley, "Transparent boundary condition for the beam propagation method," *IEEE J. Quantum Electron*., vol. 28, pp. 363-367, 1992.

[15] I. Ilić, R. Scarmozzino, R. M. Osgood, Jr., J. T. Yardley, K. W. Beeson, and M. J. McFarland, "Modeling multimode-input star couplers in polymers," *J. Lightwave Technol*., vol. 12, No. 6, pp. 996-1003, June 1994.

[16] Y. Chung, and N. Dagli, "An assessment of finite difference beam propagation method," *IEEE J. Quantum Electron*., vol. 26, No. 8, pp. 1335-1339, Aug. 1990.

[17] H. Wei, J. Yu, Z. Liu, X. Zhang, W. Shi, and C. Fang, "Fabrication of 4 × 4 tapered MMI coupler with large cross section," *IEEE Photon. Technol. Lett.*, vol. 13, No. 5, pp. 466-468, May 2001.

[18] J. A. Besley, J. D. Love, and W. Langer, "A multimode planar power splitter," *J. Lightwave Technol*., vol. 16, No. 4, pp. 678-684, April 1998.